

SCIENTIFIC REPORTS

OPEN

Subluminal group velocity and dispersion of Laguerre Gauss beams in free space

Received: 26 February 2016

Accepted: 09 May 2016

Published: 27 May 2016

Nestor D. Bareza & Nathaniel Hermosa

That the speed of light in free space c is constant has been a pillar of modern physics since the derivation of Maxwell and in Einstein's postulate in special relativity. This has been a basic assumption in light's various applications. However, a physical beam of light has a finite extent such that even in free space it is by nature dispersive. The field confinement changes its wavevector, hence, altering the light's group velocity v_g . Here, we report the subluminal v_g and consequently the dispersion in free space of Laguerre-Gauss (LG) beam, a beam known to carry orbital angular momentum. The v_g of LG beam, calculated in the paraxial regime, is observed to be inversely proportional to the beam's divergence θ_0 , the orbital order ℓ and the radial order p . LG beams of higher orders travel relatively slower than that of lower orders. As a consequence, LG beams of different orders separate in the temporal domain along propagation. This is an added effect to the dispersion due to field confinement. Our results are useful for treating information embedded in LG beams from astronomical sources and/or data transmission in free space.

Recently, Giovannini *et al.* showed through experiments, backed by calculations, that spatially structured light indeed travels slower than c within a certain path distance¹. That is, there is a decrease of group velocity v_g for structured light. Although the phenomenon can be explained classically, they used a Hong-Ou-Mandel interferometer to measure the lag of a laterally structured photon compared to a photon with little lateral structure. In their experiment, the slowing of light is due to dispersion in free space. They performed their experiment with a Bessel beam and a Gaussian beam. Alfano and Nolan remarked that by considering dispersion relation, Bessel beam can be very slow near a critical frequency which can be used as optical buffer in free space². Slowing light due to its structure is different from slowing light with materials.

Laguerre-Gauss (LG) beam is an interesting structured light since it carries orbital angular momentum (OAM). LG beam can have orders of orbital or winding order ℓ and radial order p . The scalar field of LG beam is expressed mathematically in standard cylindrical coordinates (r, φ, z) as follows,

$$\psi_{l,p}(r, \varphi) \sim r^{|\ell|} \exp\left(-\frac{r^2}{w^2(z)}\right) \exp(-i\ell\varphi) \exp\left(\frac{-ikr^2}{R(z)}\right) L_p^{|\ell|}\left(\frac{2r^2}{w^2(z)}\right) \quad (1)$$

where $L_p^{|\ell|}(x)$ is the generalized Laguerre polynomial with ℓ as integers and $p \geq 0$, $w(z) = w_0 \sqrt{1 + \frac{z^2}{z_R^2}}$ is the beam waist, $R(z) = \frac{z^2 + z_R^2}{z}$ is the radius of curvature, and $Z_R = \frac{1}{2}kw_0^2$ is the Rayleigh length³. This beam spreads along propagation as illustrated in Fig. 1a. In the far-field, the beam divergence of an $LG_{\ell=0,p=0}$ is represented by the opening angle θ_0 , which can be expressed in terms of minimum beam waist w_0 and magnitude of the wavevector k_0 as,

$$\frac{\theta_0}{2} = \frac{2}{k_0 w_0}. \quad (2)$$

In the LG expression in (1), the phase factor of the form $\ell\varphi$ means ℓ is the number of 2π windings around the azimuthal angle φ . First asserted by Allen *et al.*, these beams ($\ell \neq 0$) have Poynting vectors that spiral along the direction of propagation⁴. The helical wavefront for a beam with $\ell = 1$ is illustrated in Fig. 1b. Negative ℓ s will

National Institute of Physics, University of the Philippines Diliman, Quezon City, Diliman 1101, Philippines. Correspondence and requests for materials should be addressed to N.D.B. (email: nbareza@nip.upd.edu.ph)

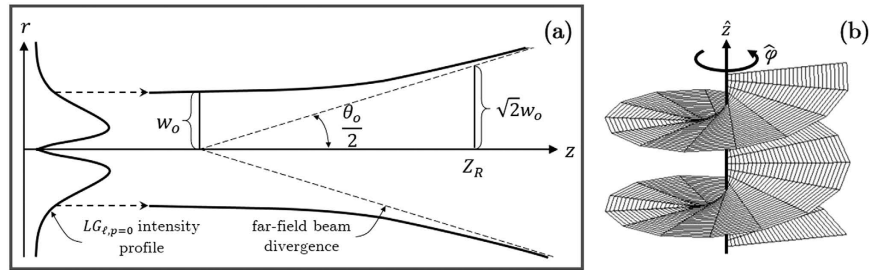


Figure 1. (a) *LG* beam spreading through propagation and (b) *LG* wavefront for $\ell = 1$ and $p = 0$.

yield the same wavefronts but of opposite helicities. The realization that *LG* beam carries OAM has led to a myriad of applications from optical tweezing and micromanipulation^{5–7}, to free space information⁸, to transverse Doppler effect⁹, and in astrophysics¹⁰.

Although the radial order p of *LG* mode is very rarely discussed, it is mostly directly used in applications. One fundamental role of p is its enhancement of the angular beam shifts in reflection of higher order *LG* beams¹¹. Moreover, higher orders of *LG* modes are also found to reduce the Brownian thermal noise in laser interferometry that could be useful in future gravitational wave detectors¹². In optical trapping, if an optical vortex due to ℓ confines atom for precision measurements, the multi-ring dislocations due to p can be used as toroidal trap in observing persistent flow of Bose-Einstein condensates^{13,14}.

In the paraxial regime, *LG* beams form a complete basis set such that it can be used as a tool in quantum information processes^{15–17}. Both ℓ and p are realized as additional degrees of freedom in encrypting information in photons^{18,19}. Hence, both the orbital and radial order can be used in encoding information aside from the polarization of the light. As an application, free-space multiplexing is possible as photons are treated with higher quantum dimensional states. Consequently, higher information density can be achieved even using the same number of photons.

In this manuscript we ask: *What is the effect of the orbital order ℓ and the radial order p of *LG* beam on its group velocity?* The consequences are extensive. The most important of which is the different time of arrival of information even in free space propagation. This is similar to the modal dispersion in fiber, a serious limitation in optical fiber communication²⁰. The promised massive information when using *LG* beams will have an issue. Information embedded in these beams will not arrive at the same time and some corrections are then necessary.

In this paper, we report our calculation on the dispersion and reduction of v_g 's in *LG* beams. The analytical expression is exact and our expression reduces to the result of Giovannini *et al.* for Gaussian beam when $\ell = 0$ and $p = 0$.

Results and Discussions

The v_g can be derived by considering geometry in the ray-optic model. The path of light follows the direction of Poynting vector which points toward the direction of the wavevector. A field confinement produces spatially structured light, which alters the wavevector to include non-axial components. The transverse components cause the delay in the v_g of light. Confined light therefore, would have its v_g that is not equal to c .

Suppose light travels along z in standard cylindrical coordinates (r, φ, z) . A plane wave has a wavevector component that is purely along z thus, this light is expected to travel at c . For Gaussian and Bessel beams, the wavevectors comprise of both longitudinal z and radial r components. The radial component will cause an added path length in the propagation of these beams. It will generate a time delay in the speed of light. For beams with OAM, the wavevectors constitute the whole basis components. The delay then for an OAM-carrying beam is due to the added path length that originated from both radial and azimuthal wavevector components.

The v_g calculation in the paraxial regime of *LG* beam is detailed in the *Methods* section. The v_g is found to be inversely proportional to the orbital order ℓ , the radial order p , and the beam's divergence θ_0 , as

$$v_g = \frac{c}{1 + \left(\frac{\theta_0}{4}\right)^2 (2p + |\ell| + 1)} \quad (3)$$

This expression shows that the delay of *LG* beam is related to its order, $2p + |\ell|$. When the order is zero, the beam reduces to a Gaussian mode ($LG_{\ell=0,p=0}$). The v_g for $\ell = 0, p = 0$ is consistent with the reported delay in Gaussian beams¹. The subluminal v_g of Gaussian modes varies for different w_0 values, and that v_g is even further reduced for relatively smaller w_0 . This holds true since, for a certain λ_0 , relatively lower w_0 yields larger far-field beam divergence. As the beam propagates for such case, the field confinement in the transverse structure is amplified.

For a fixed θ_0 , the expression results with discrete v_g values, since ℓ and p take the values of integers and natural numbers, respectively. This fact is helpful for precise detection in communications using *LG* beams, as one has prior knowledge of the beams' arrival based on discrete v_g 's.

As a representation of Equation (3), a colormap of v_g/c values for $\ell \in [-5, 5]$ and $p \in [0, 10]$, is shown in Fig. 2. We generated this plot with a beam of a central wavelength $\lambda_0 = 632.8 \text{ nm}$ and a minimum beam waist $w_0 = 2.0 \text{ }\mu\text{m}$. All values fall below unity implying subluminal speed of *LG* beams for any ℓ and p values. The case

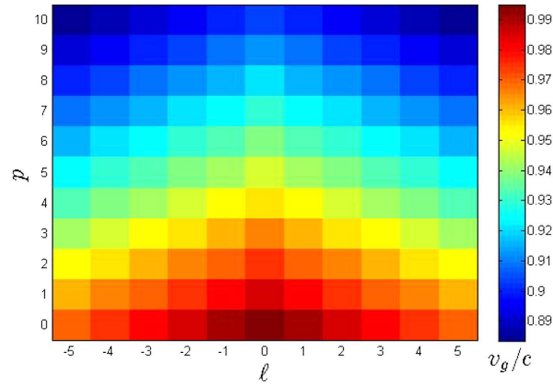


Figure 2. Colormap of v_g/c values as function of ℓ and p with central wavelength $\lambda_0 = 632.8 \text{ nm}$ and minimum beam waist $w_0 = 2.0 \mu\text{m}$. Each pixel of a specific color corresponds to v_g/c value (colored scale bar). Warm colored pixels have relatively higher v_g/c values compared to cool colored pixels.

$\ell = 0$ and $p = 0$, located at the center of lowest row, corresponds to v_g/c of a Gaussian beam. This beam obtained the largest v_g/c value or the least reduced v_g . This is expected since a Gaussian beam with no radial and orbital order is the least structured beam compared to higher modes of *LG* beams. A Gaussian beam yields the least magnitude of transverse component in the altered wavevector, hence it intuitively results with v_g closest to c .

The v_g/c becomes lower as one goes farther from $\ell = 0$ and $p = 0$, seen by the change in the color in Fig. 2. Different orders ($2p + |\ell|$) of *LG* beams disperse along propagation. The free-space dispersion based on Equation (3) can be expressed as the effective group index of refraction n_g , given by, $n_g = 1 + \left(\frac{1}{k_0 w_0}\right)^2 (2p + |\ell| + 1)$. For any w_0 values, n_g is linearly related to $2p + |\ell|$. Thus, *LG* beams of different orders that are initially propagated simultaneously will have different time delays after travelling the same path distance. This makes *LG* beams separate in the temporal domain. This contributes to the dispersion due to field confinement. A beam with higher order will have greater added path length δz , evident when relating Equation (13) to Equation (10) (see *derivation in Methods section*).

The free-space dispersion of *LG* beams consequently demands corrections in their applications such as in data transmission/communication, in multiplexing, in interaction with nonlinear materials and in OAM spectrum detection^{21–26}. The dispersion can also be substantial in quantum information processes for encryption and decryption of higher quantum dimensional states, such as ℓ and p values, in photons.

Setting $p = 0$ in Equation (3), the role of different values of OAM alone can be seen. Padgett *et al.* demonstrate that for a given beam size, the far-field opening angle increases with increasing OAM²⁷. Larger apertures are required when receiving beams with relatively higher OAM. The ℓ -dependence of v_g for *LG* beams that we report may be incorporated to such receiving optical system. A time-controllable receiving aperture size can be programmed according to computed delays prior to the arrival of beams. As opposed to the beam divergence relation presented in Equation (2) due to skewness of Poynting vector with respect to optical axis, they also considered the contribution of normal diffractive spreading by the standard deviation of the spatial distribution. They derived the far-field beam divergence α_ℓ to be dependent on $|\ell|$ whose relation is given by, $\alpha_\ell = \sqrt{\frac{|\ell| + 1}{2}} \frac{2}{k_0 w_0}$. Reformulating Equation (11), the v_g expression for OAM-carrying beams ($p = 0$) according to this beam divergence definition, we get a more compact form:

$$v_{g,p=0} = \frac{c}{1 + \frac{\alpha_\ell^2}{2}} \quad (4)$$

For light with OAM ($\ell \neq 0$) and $p = 0$, we can think that the added path length due to beam divergence increases by a factor of $|\ell| + 1$. This factor is consistent with the conservation of total linear momentum in the system. In the work of Giovannini *et al.*¹, the added path length comes from the radial component of the Poynting vector with respect to the optical axis. In Equation (13) (see *Methods section*), we show that even a Poynting vector with angular component due to ℓ with respect to the optical axis can also contribute to the path.

Figure 3a shows the plots of v_g/c versus ℓ for different p values. The symmetry of trends between $\ell < 0$ and $\ell > 0$ with respect to $\ell = 0$ shows that the dispersion of OAM-carrying beams yield the same value of v_g regardless of the helicity or polarity of ℓ . In Fig. 2, the color distributions between left and right regions mirror each other with respect to the central column, owing to the ℓ factor in Equation (3). The plot is shifted downwards for relatively higher radial order ($p > 0$). The v_g is reduced by an added $\frac{p}{(k_0 w_0)^2}$ factor in the denominator of Equation (4).

Similarly, v_g/c is plotted against p for different $|\ell|$ values in Fig. 3b. The drop in v_g/c values in these plots is steeper compared to plots of v_g versus ℓ . This is due to the 2 factor in p in Equation (3). Beams of different radial orders disperse faster than beams of different OAM. The plot of v_g/c versus p shifts downward as the beam is endowed with higher orbital order.

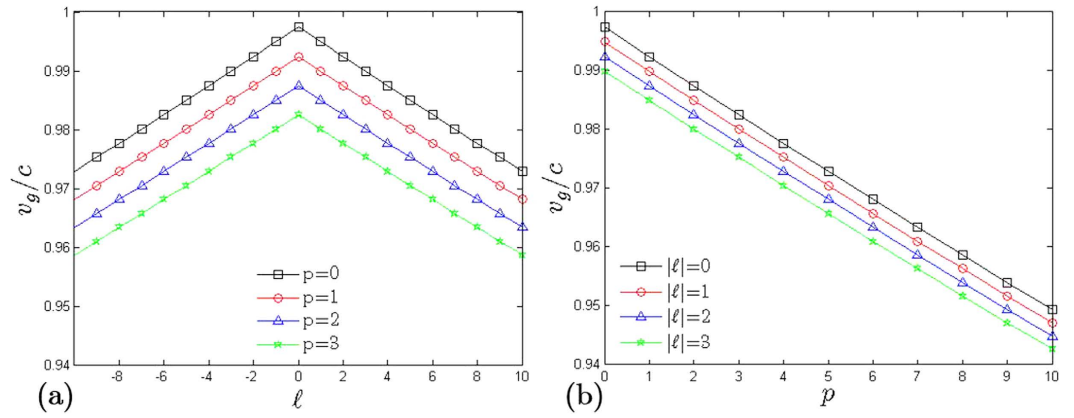


Figure 3. Plots of (a) v_g/c versus l for different p values and (b) v_g/c versus p for different l values.

Order $2p + l $	Degeneracy counts $d_{2p+ l }$	Mode indices (l, p)
1	2	(1, 0), (-1, 0)
2	3	(2, 0), (-2, 0), (0, 1)
3	4	(3, 0), (-3, 0), (-1, 1), (1, 1)
4	5	(4, 0), (-4, 0), (2, 1), (-2, 1), (0, 2)
\vdots	\vdots	\vdots

Table 1. Some combinations of mode indices yielding $2p + |l| + 1$ degenerate v_g values of LG beam in $2p + |l|$ order.

Different modes can have the same v_g as seen in Fig. 3. These modes have the same beam order but of different combinations of mode indices. We call these modes with the same v_g as degenerate modes. There will be more degenerate modes for lower v_g . This can be seen if we include more plots for higher values of p (>3) in Fig. 3a. The same can be observed in Fig. 3b by including plots with higher l 's, except that twice the modes must be accounted for $l \neq 0$ to consider the opposite helicities. Relatively higher beam order yields more degenerate modes.

The number of degenerate modes, denoted by $d_{2p+|l|}$ in the dispersion of LG beam with $2p + |l|$ order is given by,

$$d_{2p+|l|} = 2p + |l| + 1. \tag{5}$$

Only the Gaussian beam is non-degenerate, which uniquely is the fastest relative to other LG modes. The number of degenerate modes is just one plus the order of the beam. Some combinations of mode indices that yield the same v_g are presented in Table 1. In detection, the order of LG beam can be determined by performing cross correlation function even with intensity that resulted from partially coherent source²⁸. There are several ways to discriminate the explicit combination of mode indices in degeneracy of the beam order. One example is to first quantify p by employing double correlation function on the captured intensity profile²⁹. Then, the magnitude and polarity of l can be characterized by measuring OAM based on Fraunhofer diffraction pattern that is formed by passing light through shaped apertures^{30,31}.

In conclusion, we have derived the group velocity v_g of LG beam that is inversely proportional to the orbital order l , the radial order p and the far-field beam divergence θ_0 . This result shows that LG beams are both subluminal and dispersive even in free space. Discrete v_g 's are obtained for an arbitrary θ_0 . The dispersion of LG beams has degenerate modes for certain discrete v_g . The number of degenerate modes is just one plus the LG beam's order ($2p + |l|$). We also highlight that light travels in the direction of the Poynting vector, therefore both radial and angular components will contribute to the added path length. This report would have far-reaching consequences on the OAM beam's applications.

Methods

The transverse wavevector of a light beam alters both the phase velocity v_p and group velocity v_g . We are only concern with v_g calculation since this parameter corresponds to the actual speed of light as it travels through space, whereas v_p indicates the field signal variation³².

For a given path length Δz between two different points such as z_1 and z_2 , a structured light travels at a time Δt that includes an added path length δz due to the transverse components of the wavevector. They are related by $\Delta t = (\Delta z + \delta z)/c$. In the ray-optic model, the v_g can be obtained by calculating δz and is mathematically formulated as follows,

$$v_g = \frac{c}{\left(1 + \frac{\delta z}{\Delta z}\right)}. \quad (6)$$

The path of light can be represented as a diverted ray with a certain angle from the beam axis. The amount of δz is the difference between length of diverted ray within the actual path and Δz . This can be expressed as

$$\delta z = \left[\left(\frac{\partial \Phi}{\partial k} \right)_{k_0} - z \right]_{z_1}^{z_2} \quad (7)$$

where Φ is the phase profile of the scalar field. As an example, $\Phi = kz - \omega t$ for plane wave thus δz is zero, as expected. However for *LG* beam, the beam waist varies significantly at distances near the Rayleigh length. This manifests variation of v_g as it propagates in the near field. We consider the paraxial regime in order to simplify further δz , so that we can derive an expression of z -independent v_g for any arbitrary field. This then translates spatial dependence of v_g into wavevector. The derivation by Giovannini *et al.*¹ considers Φ as complex argument of the scalar field function,

$$\Phi = \arg\langle \psi(z, k_0) | \psi(z, k) \rangle. \quad (8)$$

The paraxial wave equation is then written in terms of quantum mechanical operator with evolution of wavefunction from z_1 to z_2 :

$$|\psi(z_2, k)\rangle = \exp\left[\Delta z \left(\frac{i}{2k} \nabla_{\perp}^2 + ik \right)\right] |\psi(z_1, k)\rangle \quad (9)$$

where $\hat{k}_{\perp} = -i \nabla_{\perp}$ is the operator representing the transverse wave vector. By taking an inner product of $\psi(z_2, k)$ in Equation (9) and substituting the result to Equation (7), we obtain the relation:

$$\frac{\delta z}{\Delta z} = \frac{\langle \hat{k}_{\perp}^2 \rangle}{2k_0^2} \quad (10)$$

so that Equation (6) becomes,

$$v_g = \frac{c}{1 + \frac{\langle \hat{k}_{\perp}^2 \rangle}{2k_0^2}} \quad (11)$$

where,

$$\langle \hat{k}_{\perp}^2 \rangle = \frac{\langle \psi | \hat{k}_{\perp}^2 | \psi \rangle}{\langle \psi | \psi \rangle} = - \frac{\langle \psi | \nabla_{\perp}^2 | \psi \rangle}{\langle \psi | \psi \rangle} \quad (12)$$

such that ∇_{\perp}^2 operator is the transverse Laplacian.

Now, for an *LG* beam, we substitute Equation (1) to Equation (12) in order to have

$$\langle k_{\perp}^2 \rangle = \frac{2}{w_0^2} (2p + |\ell| + 1). \quad (13)$$

And the group velocity for such beam is given by,

$$v_g = \frac{c}{1 + \left(\frac{1}{k_0 w_0}\right)^2 (2p + |\ell| + 1)} \quad \text{or,} \quad v_g = \frac{c}{1 + \left(\frac{\theta_0}{4}\right)^2 (2p + |\ell| + 1)} \quad (14)$$

where $1/k_0 w_0$ is replaced by the opening angle of the beam $\theta_0/4$ for a more intuitive picture. When $\ell = 0$ and $p = 0$,

$$v_g = \frac{c}{\left(1 + \frac{1}{k_0^2 w_0^2}\right)}. \quad (15)$$

Equation (15) is consistent with the calculation for Gaussian beam¹.

References

1. Giovannini, D. *et al.* Spatially structured photons that travel in free space slower than the speed of light. *Science* **347**, 857–860 (2015).
2. Alfano, R. R. & Nolan, D. A. Slowing of bessel light beam group velocity. *Opt. Commun.* **361**, 25–27 (2016).
3. Mazilu, M. & Dholakia, K. *Twisted photons: applications of light with orbital angular momentum* (eds Torres, J. P., Torner, L.) Ch. 4, 37–62 (John Wiley & Sons, 2011).
4. Allen, L., Beijersbergen, M. W., Spreeuw, R. & Woerdman, J. Orbital angular momentum of light and the transformation of laguerre-gaussian laser modes. *Phys. Rev. A* **45**, 8185 (1992).
5. Curtis, J. E., Koss, B. A. & Grier, D. G. Dynamic holographic optical tweezers. *Opt. Commun.* **207**, 169–175 (2002).

6. Galaja, P. *et al.* *Twisted photons: applications of light with orbital angular momentum* (eds Torres, J. P., Torner, L.) Ch. 7, 117–139 (John Wiley & Sons, 2011).
7. Simpson, N., Dholakia, K., Allen, L. & Padgett, M. Mechanical equivalence of spin and orbital angular momentum of light: an optical spanner. *Opt. Lett.* **22**, 52–54 (1997).
8. Gibson, G. *et al.* Free-space information transfer using light beams carrying orbital angular momentum. *Opt. Express* **12**, 5448–5456 (2004).
9. Rosales-Guzmán, C., Hermosa, N., Belmonte, A. & Torres, J. P. Experimental detection of transverse particle movement with structured light. *Sci. Rep.* **3** (2013).
10. Berkhout, G. C. & Beijersbergen, M. W. Method for probing the orbital angular momentum of optical vortices in electromagnetic waves from astronomical objects. *Phys. Rev. Lett.* **101**, 100801 (2008).
11. Hermosa, N., Aiello, A. & Woerdman, J. Radial mode dependence of optical beam shifts. *Opt. Lett.* **37**, 1044–1046 (2012).
12. Chelkowski, S., Hild, S. & Freise, A. Prospects of higher-order laguerre-gauss modes in future gravitational wave detectors. *Phys. Rev. D* **79**, 122002 (2009).
13. Kennedy, S. A., Szabo, M. J., Teslow, H., Porterfield, J. Z. & Abraham, E. Creation of laguerre-gaussian laser modes using diffractive optics. *Phys. Rev. A* **66**, 043801 (2002).
14. Ryu, C. *et al.* Observation of persistent flow of a bose-einstein condensate in a toroidal trap. *Phys. Rev. Lett.* **99**, 260401 (2007).
15. Mair, A., Vaziri, A., Weihs, G. & Zeilinger, A. Entanglement of the orbital angular momentum states of photons. *Nature* **412**, 313–316 (2001).
16. D'Ambrosio, V., Nagali, E., Marrucci, L. & Sciarrino, F. Orbital angular momentum for quantum information processing. In *SPIE Photonics Europe, 84400F–84400F* (International Society for Optics and Photonics, 2012).
17. Molina-Terriza, G., Torres, J. P. & Torner, L. Twisted photons. *Nat. Phys.* **3**, 305–310 (2007).
18. Karimi, E. *et al.* Exploring the quantum nature of the radial degree of freedom of a photon via hong-ou-mandel interference. *Phys. Rev. A* **89**, 013829 (2014).
19. Djordjevic, I. B. Deep-space and near-earth optical communications by coded orbital angular momentum (oam) modulation. *Opt. Express* **19**, 14277–14289 (2011).
20. Verdeyen, J. T. *Laser electronics* (Englewood Cliffs, NJ, Prentice Hall, 1989).
21. Wang, J. *et al.* Terabit free-space data transmission employing orbital angular momentum multiplexing. *Nat. Photonics* **6**, 488–496 (2012).
22. Karimi, E., Marrucci, L., de Lisio, C. & Santamato, E. Time-division multiplexing of the orbital angular momentum of light. *Opt. Lett.* **37**, 127–129 (2012).
23. Tamburini, F. *et al.* Encoding many channels on the same frequency through radio vorticity: first experimental test. *New J. Phys.* **14**, 033001 (2012).
24. Steinlechner, F., Hermosa, N., Pruneri, V. & Torres, J. P. Frequency conversion of structured light. *Sci. Rep.* **6**, 21390 (2016).
25. Boyd, R. W. *Nonlinear optics* (Academic press, 2003).
26. Lavery, M. P. *et al.* Efficient measurement of an optical orbital-angular-momentum spectrum comprising more than 50 states. *New J. Phys.* **15**, 013024 (2013).
27. Padgett, M. J., Miatto, F. M., Lavery, M. P., Zeilinger, A. & Boyd, R. W. Divergence of an orbital-angular-momentum-carrying beam upon propagation. *New J. Phys.* **17**, 023011 (2015).
28. Yang, Y. *et al.* Effect of the radial and azimuthal mode indices of a partially coherent vortex field upon a spatial correlation singularity. *New J. Phys.* **15**, 113053 (2013).
29. Yang, Y. & Liu, Y.-d. Measuring azimuthal and radial mode indices of a partially coherent vortex field. *J. Opt.* **18**, 015604 (2015).
30. Hickmann, J., Fonseca, E., Soares, W. & Chávez-Cerda, S. Unveiling a truncated optical lattice associated with a triangular aperture using light's orbital angular momentum. *Phys. Rev. Lett.* **105**, 053904 (2010).
31. Guo, C.-S., Lu, L.-L. & Wang, H.-T. Characterizing topological charge of optical vortices by using an annular aperture. *Opt. Lett.* **34**, 3686–3688 (2009).
32. Griffiths, D. J. & College, R. *Introduction to electrodynamics* vol. 3 (prentice Hall Upper Saddle River, NJ, 1999).

Acknowledgements

This work is supported by the University of the Philippines Office of the Vice-President for Academic Affairs thru its Balik-PhD program (OVPA-BPhD 2015-06).

Author Contributions

N.H. and N.D.B. equally contributed to the research. N.H. provided the initial problem. N.D.B. made the calculations. Both contributed to the analysis of the results.

Additional Information

Competing financial interests: The authors declare no competing financial interests.

How to cite this article: Bareza, N. D. and Hermosa, N. Subluminal group velocity and dispersion of Laguerre Gauss beams in free space. *Sci. Rep.* **6**, 26842; doi: 10.1038/srep26842 (2016).



This work is licensed under a Creative Commons Attribution 4.0 International License. The images or other third party material in this article are included in the article's Creative Commons license, unless indicated otherwise in the credit line; if the material is not included under the Creative Commons license, users will need to obtain permission from the license holder to reproduce the material. To view a copy of this license, visit <http://creativecommons.org/licenses/by/4.0/>